Ultrafast electron dynamics in a metallic quantum well nanofilm with spin splitting

A. Ruffing,[1] S. Vollmar,[1,2] S. Jakobs,[1,2] S. Kaltenborn,[1] A. Baral,[1] M. Cinchetti,[1] S. Mathias,[1,*] H. C. Schneider,[1] and M. Aeschlimann[1]

[1]*University of Kaiserslautern and Research Center OPTIMAS, 67663 Kaiserslautern, Germany*

[2]*Graduate School Materials Science in Mainz, Erwin Schroedinger Straße 46, 67663 Kaiserslautern, Germany*

(Received 18 December 2012; revised manuscript received 25 July 2013; published 30 August 2013)

Using time- and angle-resolved two-photon photoemission spectroscopy, we investigate the energy- and momentum-dependent ultrafast electron dynamics in the Rashba spin-split quantum-well nanofilm Bi/Cu(111). We find an expected increase of electron lifetimes towards the band bottom due to a competition of intra- and interband scattering processes. In addition, we find an unexpected peculiar decrease of the lifetimes around the intersection of the split bands. We compare the experimental results with calculated lifetimes due to electron-electron scattering in a model system of a 2D electron gas including a Rashba interaction term and an effective statically screened Coulomb interaction. Although the Rashba model reproduces the increase of lifetimes towards the band bottom well, there is no indication of the experimentally observed decrease around the intersection point in this simple model system. To investigate spin-orbit coupling effects, beyond those contained in a pure Rashba model, we introduce a phenomenological k-dependent spin mixing that leads to a "spin hot spot." It is shown that such a mixing would strongly increase the electron-electron scattering rate around the band intersection and thus improves the agreement with experiment.

DOI: 10.1103/PhysRevB.88.075148 PACS number(s): 71.70.Ej, 78.47.J−, 73.50.Gr, 73.20.At

I. INTRODUCTION

New materials with large spin-orbit coupling show promise for potential applications in the area of spintronic devices. A particularly important spin-orbit coupling effect is the Rashba-Bychkov effect[1] in a two-dimensional electron gas, which needs an asymmetric confinement of the electron gas and gives rise to spin-split energy bands in nonmagnetic materials without the need to apply an external magnetic field. A large Rashba splitting of the spin-polarized electronic bands is favorable for potential applications[2] and has been found at various surfaces,[3] in quantum wells,[4–6] and at the surfaces of new materials, i.e., topological insulators.[7] Very recently, for instance, extremely strong spin-orbit splittings have been found in BiTeI[8,9] and BiTeCl.[10] For the purpose of applications, but also from a fundamental point of view, it is of importance to understand the consequences of spin-orbit coupling and splitting on the electronic (spin-)dynamics, electron lifetimes, and according spin-diffusion lengths. The Rashba spin splitting can serve as a comparatively simple model system for general spin-orbit coupling effects.

In this paper, we use time- and angle-resolved two-photon photoemission spectroscopy (tr-2PPE) to study energy- and momentum-dependent electron-electron scattering processes around the intersection of spin-split electron bands. The measurements have been carried out on the Bi/Cu(111) quantum-well system, where spin splitting in the unoccupied regime of the band structure has been previously assigned to the Rashba effect.[4] Using tr-2PPE, we can access the electron dynamics in these spin-split electronic bands and show that the electron lifetimes are strongly influenced by the competition of inter- and intraband scattering processes, however, with a peculiar lifetime plateau around the intersection of the Rashba bands. To understand this for a metal atypical energy and momentum dependencies, we calculate the electronic lifetimes due to electron-electron scattering in a two-dimensional electron gas including a Rashba interaction with effective Rashba parameters derived from experiment. Furthermore, we determine the static screening properties of the metallic QW system. Although the calculated lifetimes match the experimentally observed lifetimes quite well, the interesting behavior near the intersection point cannot be reproduced, and we conclude that spin-orbit coupling effects beyond those described in a pure Rashba model must play a role in the Bi/Cu(111) system. Finally, we attribute the origin of the decreased lifetime around the intersection point to a higher probability of scattering processes in the spin-split bands. For our simulations, in order to amplify the scattering decay rate, we need to introduce a phenomenological k-dependent spin mixing around the intersection point, which is equivalent to a so-called spin hot spot.[11,12]

II. EXPERIMENT

A. Time- and angle-resolved 2-photon photoemission

Figure 1(a) displays a static angle-resolved 2PPE spectrum of the quantum-well system 1 monolayer (ML) Bi/Cu(111) as a function of intermediate state energy $E - E_F$ and k vector parallel to the surface, $k_\parallel$, in $\overline{\Gamma}$-$\overline{\mathrm{M}}$ direction, as observed previously.[4] All measurements have been carried out at liquid nitrogen temperature. The calculation of the parallel momentum $k_\parallel$ has been carried out following the approach in Ref. 13 in order to take the sample-analyzer bias voltage of 2 V into account. A detailed characterization of the system and the experimental setup is given in Refs. 4 and 14. The spectrum is measured with two photons with energy $h\nu = 3.12$ eV, each. The first light pulse excites electrons from below the Fermi-level into the unoccupied spin-split quantum-well band structure between Fermi and vacuum level. The second pulse then excites these electrons from the unoccupied electronic structure into the vacuum [see Fig. 1(d)], where the electronic energy and momentum are detected using an angle-resolved photoelectron analyzer.

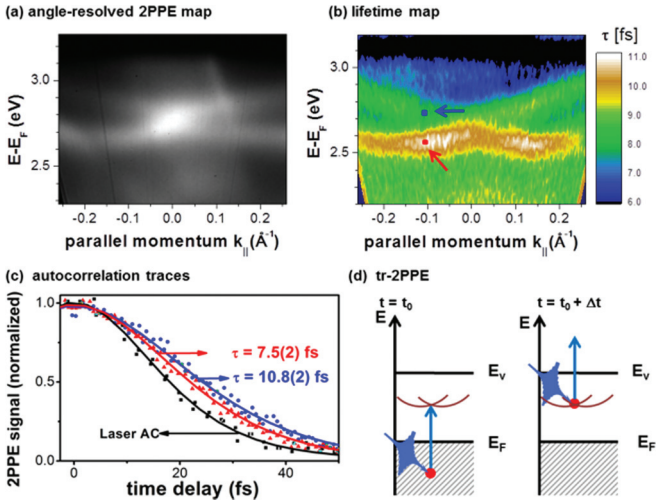

FIG. 1. (Color online) (a) 2PPE map of the spin-split electron bands from angle-resolved 2PPE in a commensurate overlayer Bi/Cu(111). The gray scale represents photoemission intensity. (b) Corresponding inelastic lifetime map $\tau(E,k_\parallel)$ of the spin-split electron bands from angle-resolved tr-2PPE. The lifetime τ is color coded as a function of energy E and parallel momentum $k_\parallel$. Both spectra have been recorded for a series of emission angles and stitched here for qualitative illustration.[15] Note that the photoemission spectrum (a) has been collected with a narrow-bandwidth Ti:sapphire oscillator ($\Delta E = 20$ meV, pulse length >100 fs), and the time-resolved data in (b) with a broad-bandwidth short-pulse Ti:sapphire oscillator [$\Delta E = 100(5)$ meV, pulse length ≈27 fs]. (c) Exemplary autocorrelation traces (symbols) with fits (lines) extracted from the red and blue marked areas in Fig. 1(b), however, from the nonstitched raw data, in comparison to the laser-autocorrelation trace. (d) Schematic of the time-resolved 2PPE process. Δt is the temporal delay between the pulses.

The observed quantum-well paraboliclike dispersion shows the signature of a Rashba-type spin-orbit splitting in $k_\parallel$ direction.[4] The intersection of the dispersive quantum-well parabola at the $\overline{\Gamma}$ point is located at an energy between Fermi and vacuum levels of $E - E_F = 2.76(1)$ eV for Fig. 1(a), and $E - E_F = 2.65(2)$ eV for Fig. 1(b). Note that this value differs since the energetic position depends critically on the exact commensurate wetting layer thickness and shifts up to 100 meV depending on the fabrication and tempering process, which, however, does not influence the observed electron dynamics as reported below.

In the next step, we use tr-2PPE to measure the electron lifetimes in the complete Rashba spin-split band structure. Tr-2PPE data are collected in autocorrelation mode using identical p-polarized laser pulses of energy $h\nu = 3.12$ eV and ≈27 fs pulse lengths. Interference contributions to the signal are phase averaged during acquisition using an electric-wobbling motor. Then, a series of angle-resolved 2PPE photoemission maps is recorded as a function of temporal delay Δt between the two laser pulses [see Fig. 1(d)]. From these data, i.e., $E(k_\parallel)$ intensity maps as a function of delay, individual semioverlapping $I(\Delta E, \Delta k_\parallel)$ 2PPE autocorrelation traces are extracted, with I the photoemission intensity, $\Delta E = 40$ meV, and $\Delta k_\parallel = 0.01$ Å^{-1} (in comparison to $\Delta E =$ 100 meV and $\Delta k_\parallel = 0.03$ Å^{-1} experimental resolution, more details are given in Ref. 14). Exemplary $I(\Delta E, \Delta k_\parallel)$ 2PPE autocorrelation traces extracted from the indicated areas in Fig. 1(b) are displayed in Fig. 1(c). The hot-electron lifetimes are then deconvoluted following the approach described in Refs. 16 and 17. This deconvolution procedure yields an inelastic electron-lifetime data set, $\tau(E,k_\parallel)$, which is displayed in Fig. 1(b). Here, the color-code represents the hot-electron lifetime as a function of E and $k_\parallel$ [rather than photoemission intensity as in Fig. 1(a)]. Since the data are collected in a parallel detection scheme, we achieve very low relative errors of the deconvoluted lifetimes within the lifetime map. The deconvoluted lifetime errors from the fitted autocorrelation traces [see solid lines in Fig. 1(c)] yield values of about ±200 as. Overall, we therefore give an upper limit of the relative error of ±250 as. One color-step in Fig. 1(b) is 100 as. The absolute experimental error of the complete lifetime map is about 2 fs, determined by the accuracy of the laser-pulse duration, which is extracted by the measurement of the 2PPE autocorrelation trace for excitation from the Cu(111) Shockley surface state [black data points and corresponding fit to autocorrelation trace in Fig. 1(c)].[18] Additionally, the absolute values critically depend on the exact model used to fit the lifetime-broadened autocorrelation traces. Here, however, we focus on the relative energy and momentum dependence of the hot-electron lifetimes in the vicinity of the Rashba intersection point.

B. Experimental results

Figure 1(b) clearly shows an energy dependence of the lifetimes, which is influenced by the details of the band structure. The longest lifetimes are found at the minima of the spin-split parabolic bands, as expected. Surprisingly, however, there is an unusual pronounced variation of the electron lifetimes around the intersection point. Next, we display in Fig. 3 the deconvoluted lifetimes in the spin-split parabolic Rashba bands as a function of $E - E_F$. According values from positive and negative momentum vectors have been averaged to account for the slight asymmetry for positive and negative momentum vectors as seen in the lifetime map in Fig. 1(b). In the small area of about ±0.01 Å^{-1} around the Γ point, we cannot resolve the individual Rashba bands due to the limited energy resolution ($\Delta E = 20$ meV for the static spectra). We therefore set upper limits to the possible dispersion of the parabolic Rashba bands in this intersection area from the values extracted by peak fitting at higher momentum vectors. To account for this procedure, we indicate increased error bars of ±20 meV around the intersection energy at $E - E_F \approx 2.65(2)$ eV in Fig. 3. We emphasize that the unusual pronounced variation of the lifetimes around the intersection point is seen up to momentum vectors of about ±0.15 Å^{-1}, and does therefore not result from the uncertainty of the estimated band dispersion. We note, however, that the energy resolution in the time-resolved data sets measured with the pulse length ≈27 fs laser system is worse, i.e., $\Delta E = 100(5)$ meV, which indeed does influence the extracted lifetime values (as discussed below), but not strong enough to account for the observed dynamics. Finally, in Fig. 3, red and blue circles display the extracted electron lifetimes in the

bands from Fig. 1(b) below and above the intersection point, respectively, as a function of energy $E - E_F$.

Before we discuss the lifetime dependence in detail, we need to introduce the electron-electron scattering processes, which determine the finite lifetime of the excited electrons. In the following, we will refer to the unoccupied spin-split bands as Rashba bands. For electron-electron scattering, one generally distinguishes between interband- and intraband-scattering processes. Since the Rashba bands are never appreciably populated, i.e., on average, less than one electron is photoemitted per pulse, the interaction between electrons in the Rashba bands can be neglected. Thus the hot electrons must relax their energy via Coulomb scattering with electrons in a different band below the Fermi level. The scattering partner in this relaxation process gains energy from the hot electron and is excited into an unoccupied state.

For intraband-scattering processes, excited electrons remain inside the Rashba bands but change their momentum and cascade in energy down towards a band minimum. Note that the spin structure reduces the possible scattering paths. In interband-scattering processes, the excited electrons are scattered out of the Rashba bands.

Interband-scattering processes follow approximately a Fermi-liquid lifetime dependence. However, around energies of about 2.5–3.0 eV above the Fermi level, where the spin-split Rashba bands studied here in this paper are located, the *interband* scattering rate varies by less than 1 fs.[14,19] The observed momentum dependence of the electronic lifetimes in the Rashba bands is therefore mostly determined by the efficiency of *intraband* scattering processes. For intraband scattering, the available phase-space gradually decreases when approaching a band minimum. Consequently, the lifetime increases towards lower energies as seen in Fig. 3 (red and blue circles). This behavior of electron dynamics in parabolic bands is, of course, well known.[14,20–22] A single (spin-polarized) parabolic band should show the longest lifetime at the minimum of the band, but with a smooth and regular lifetime dependence towards higher energies and momenta. However, for the Rashba system studied here, we find a pronounced variation of the electron lifetimes in the energy range of about 150 meV around the Rashba intersection point, which is located at $E - E_F = 2.65(2)$ eV. In the present study, we will focus on this peculiar feature more closely.

First, we note that the decrease of the lifetimes coincides with the highest intensity in the photoemission spectrum at the intersection point. Such high intensity could arise from a direct 2PPE transition from a localized initial state, which might influence the full width at half maximum (FWHM) of the extracted autocorrelation traces.[23,24] However, we can exclude such a direct excitation, since no localized initial state is present in the respective energy and momentum range.[4]

After excluding such an artificial contribution, we would like to start our discussion with a short survey of possible mechanisms that might increase the electron-electron scattering rate around the intersection point as observed in our experiment. In order to reproduce such dynamics, we need either (i) a strong variation of the interband-scattering rate, (ii) a strong variation of the intraband-scattering rate, or (iii) an additional decay channel that opens up in the particular $E(k_\parallel)$ range. For the latter, resonant electron transfer to the bulk might be a possible process[19,22,25,26] that could decrease the electron lifetimes, which we, however, can exclude here, since the investigated Rashba states are fully localized in the Cu(111) projected bulk band gap. Also, the interband-scattering rate (i) to the bulk only shows a very small and smooth lifetime reduction towards higher energies in the energy range investigated here[14,19,22] and does not exhibit any additional $k_\parallel$ dependence.[22,27] Therefore finding the highest lifetimes exactly at the bottom of the spin-split parabolas at *finite* $k_\parallel$ values very strongly indicates that variations in the intraband-scattering rate (ii) dominate the band-structure-dependent electron dynamics observed here (reduction of phase-space when approaching a band minimum).

III. THEORETICAL MODEL

A. Electronic states and lifetimes

To contribute to an understanding of the experimentally observed properties of electronic lifetimes in this spin-split system, we calculate the lifetime due to electron-electron scattering in a simple, semiempirical model designed to capture essential aspects of the system under study. Our model consists of a 2D electron gas with a Rashba spin-orbit-coupling and the Coulomb interaction between the carriers. As mentioned above, the hot electrons in the Rashba band reduce their energy via Coulomb scattering with a second electron in a different band. The respective spin structure of the Rashba bands thereby reduces the possible scattering paths. To model these scattering transitions, we include in the calculation the parabolic occupied QW state of the Bi/Cu(111) system (as shown in Ref. 4), which can be expected to contribute most effectively to the scattering processes due to the high wave-function overlap between initial and final states,[28,29] localized in the ultrathin Bi film. As mentioned above, the contribution due to interband-scattering processes is fairly constant at such high energies above the Fermi level,[14] and therefore also kept constant in the calculation for the investigated energy range.

We use a standard linearized Rashba Hamiltonian for electronic states confined in the xy-plane with Rashba parameter $\alpha = 200$ meVnm and effective mass $m_1^* = 0.34\, m_e$ determined from experimental data:

$$H = H_0 + H_{\text{Rashba}} = \frac{\hbar^2 k^2}{2m_1^*} + \alpha(k_y\sigma_x - k_x\sigma_y) + E_\Delta. \quad (1)$$

The energy offset $E_\Delta = 2.65$ eV reproduces the energetic position of the crossing point and is also extracted from experiment. This Hamiltonian leads to energies

$$E_\sigma(k) = \frac{\hbar^2 k^2}{2m_1^*} + \sigma\alpha k + E_\Delta \quad (2)$$

and single-electron states

$$|\mathbf{k},\sigma\rangle = \frac{1}{\sqrt{2}}\begin{pmatrix} \sigma i e^{-i\varphi_{\mathbf{k}}} \\ 1 \end{pmatrix}. \quad (3)$$

Here, we denote by $\sigma = +,-$ the different Rashba bands as shown in Fig. 2(a). The energies depend only on the modulus of $|\mathbf{k}|$, i.e., the energy dispersion is isotropic. Figure 2(b) shows the spin orientation in the Rashba bands. For the lifetime

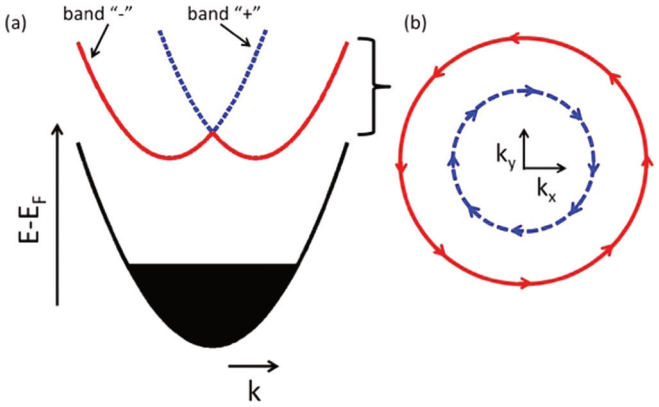

FIG. 2. (Color online) (a) Energy dispersion of the Rashba bands and the filled parabolic band. (b) In-plane spin orientation in a Rashba system.

calculation, we model the scattering partners of the excited electrons in the Rashba bands by an occupied parabolic band

$$\varepsilon(k) = \frac{\hbar^2 k^2}{2m_2^*} + \varepsilon_{\min}, \tag{4}$$

which is seen in experiments on the Bi/Cu(111) system.[4] Because of the strong localization in the ultrathin Bi film, we assume that the electrons in this band are the most efficient scattering partners. The parameters $m_2^* = 0.24\,m_e$ and $\varepsilon_{\min} = -1.24$ eV are extracted from experiment.

The expression for the inverse lifetime[30,31]

$$\begin{aligned}\tau_\sigma^{-1}(k) = \frac{2\pi}{\hbar}\sum_{\mathbf{l},\mathbf{q}}\sum_{\mu}\left(V_q^S\right)^2 |\langle \mathbf{k},\sigma|\mathbf{k}+\mathbf{q},\mu\rangle|^2 \\ \times \delta[E_\sigma(k) - E_\mu(|\mathbf{k}+\mathbf{q}|) + \varepsilon(|\mathbf{l}+\mathbf{q}|) - \varepsilon(l)] \\ \times (1-f(l))f(|\mathbf{l}+\mathbf{q}|)\end{aligned} \tag{5}$$

can be obtained from a linearized Boltzmann scattering integral, where $f(p) = f(\varepsilon(p))$ is the Fermi-Dirac distribution of the electrons in the parabolic band. In writing this expression we have assumed a statically screened Coulomb potential and that the scattering partners of the excited electrons in the Rashba band are in the parabolic band, see Fig. 2(a). The square of the absolute value of the matrix element

$$M_{\mathbf{k},\mathbf{q}}^{\sigma,\mu} = |\langle \mathbf{k},\sigma|\mathbf{k}+\mathbf{q},\mu\rangle|^2 = \tfrac{1}{2}[1+\sigma\mu\cos(\vartheta)] \tag{6}$$

gives the transition probability from the initial state of the excited electron to its final state.

For the linearized Rashba model, this matrix element only depends on the band indices σ,μ, and the angle ϑ between the momentum vectors $\mathbf{k}$ of the initial and final states. The statically screened Coulomb potential is denoted by V_q^S. The form of this potential in the Bi layer in the xy plane on a copper substrate with the normalization area A,

$$V_q^S = \frac{e^2}{2A\varepsilon_0\sqrt{q^2+\kappa_{\mathrm{Cu}}^2}+q}, \tag{7}$$

is determined by the screening properties of the whole structure and examined in some detail in the next section. κ_{Cu} is the 3D static screening parameter of the copper substrate.

B. Interaction potential

For the derivation of Eq. (7), we solve the Poisson equation

$$-\varepsilon_0\nabla^2\Phi(\mathbf{r}) = \rho_{\mathrm{ext}} + \rho_{\mathrm{ind}} \tag{8}$$

for the electrostatic potential $\Phi(\mathbf{r})$ with an externally controlled charge at $\vec{r} = \vec{0}$, taken to be

$$\rho_{\mathrm{ext}} = e\delta(\mathbf{r}). \tag{9}$$

The induced charge density is expressed by the density of states of bismuth at the Fermi edge $D_{\mathrm{Bi}}(E_F)$,

$$\rho_{\mathrm{ind}} = -e^2 D_{\mathrm{Bi}}(E_F)\Phi(\mathbf{r}). \tag{10}$$

We choose coordinates such that the z axis is normal to the film and such that the x/y axes lie in the plane of the Bi film and assume for now a finite extension of the film from $z = -d$ to d. After a two-dimensional Fourier transformation in the plane, the Poisson equation takes the form

$$\left(\partial_z^2 - q^2 - \kappa_{\mathrm{Bi}}^2\right)\Phi(\vec{q},z) = -\frac{e}{\varepsilon_0}\delta(z), \tag{11}$$

with the two-dimensional wave vector $\vec{q} = (q_x,q_y)$ and the screening constant $\kappa_{\mathrm{Bi}}^2 = \frac{e^2}{\varepsilon_0}D_{\mathrm{Bi}}(E_F)$ in the bismuth layer. The general solution for the potential in the layer is (with the definition $q_{\mathrm{Bi}} = \sqrt{q^2+\kappa_{\mathrm{Bi}}^2}$)

$$\begin{aligned}\Phi(\vec{q},z) = \frac{e}{\varepsilon_0}[e^{q_{\mathrm{Bi}}z}\Theta(-z) + e^{-q_{\mathrm{Bi}}z}\Theta(z)] \\ + \Phi_- e^{-q_{\mathrm{Bi}}z} + \Phi_+ e^{q_{\mathrm{Bi}}z}.\end{aligned} \tag{12}$$

Here, $e^{\pm q_{\mathrm{Bi}}z}$ are homogenous solutions to the differential operator in Eq. (11) that are added to the inhomogeneous solutions of Eq. (11), and $\Phi_\mp$ (Θ denotes the Heavyside step function) have to be determined from the boundary conditions. Further, we assume solutions of the homogenous Poisson equation in the vacuum above the layer

$$\Phi_{\mathrm{Vac}}(\vec{q},z) = \Phi_0 e^{-qz} \tag{13}$$

and in the copper substrate below ($q_{\mathrm{Cu}} = \sqrt{q^2+\kappa_{\mathrm{Cu}}^2}$)

$$\Phi_{\mathrm{Cu}}(\vec{q},z) = \Phi_1 e^{q_{\mathrm{Cu}}z}. \tag{14}$$

Requiring the potential and its derivative to be continuous at the boundaries of the layer $z = d$ and $-d$ fixes Φ_-, Φ_+, Φ_0, and Φ_{Vac}. Because the screening in bismuth is very small with $\kappa_{\mathrm{Bi}} \approx 0.05\mathrm{nm}^{-1}$,[32] and because the thickness of the layer is a few angstroms, we assume $e^{-2\kappa_{\mathrm{Bi}}d} \approx e^{2\kappa_{\mathrm{Bi}}d} \approx 1$. This leads to the potential in Eq. (7) and shows that the thin Bi film effectively does not contribute to the screening.

By using the statically screened interaction as in Eq. (7) in the lifetime expression of Eq. (5), we include important aspects of the screening behavior in the layered structure. We neglect dynamical aspects of the screening as studied, e.g., in Ref. 33 that may arise from plasmon resonances of the electron gas in the Rashba bands. There is no indication of a plasmon resonance in the energy range considered here so that the static screening should be sufficient to determine the energy dependence of the lifetimes.

C. Numerical examination

The numerical evaluation of Eq. (5) is done in the form

$$\tau_\sigma^{-1}(k) = -\frac{2}{\hbar}\sum_{\mathbf{q}}\sum_{\mu}\left(V_q^S\right)^2 |\langle \mathbf{k},\sigma|\mathbf{k}+\mathbf{q},\mu\rangle|^2 \times b(\hbar\omega)\chi''(\mathbf{q},\hbar\omega), \quad (15)$$

where $\hbar\omega = E_\mu(|\mathbf{k}+\mathbf{q}|) - E_\sigma(k)$ is the transferred energy, $b(\hbar\omega)$ is the Bose-Einstein distribution function, and $\chi''(\mathbf{q},\hbar\omega)$ the imaginary part of the susceptibility for the parabolic band:[34,35]

$$\chi''(\mathbf{q},\hbar\omega) = \frac{1}{2\pi}\frac{m_2^*}{\hbar^2 q}\left[\Theta(k_F - k_+)\sqrt{k_F^2 - k_+^2} - \Theta(k_F - k_-)\sqrt{k_F^2 - k_-^2}\right] \quad (16)$$

with

$$k_\pm = \left|\frac{m_2^*}{\hbar^2 q}(\varepsilon(q) \pm \hbar\omega)\right|. \quad (17)$$

As mentioned above, experimentally it is well established that there is an interband contribution to the lifetime that prevents the excited carriers from piling up at the bottom of the Rashba bands. Since this contribution is nearly constant in the energy range considered here, we take this contribution into account by writing

$$\tau_{\sigma,\mathrm{tot}}^{-1}(k) = \tau_\sigma^{-1}(k) + \Gamma_{\mathrm{inter}}, \quad (18)$$

where $\Gamma_{\mathrm{inter}} = (10.8\ \mathrm{fs})^{-1}$ is determined by the measured lifetime at the band bottom.

D. Results

We first investigate whether our idealized Rashba system can explain the observed dynamics. The black solid line in Fig. 3(a) shows the calculated results compared to the experimental data. For a screening constant of $\kappa_{\mathrm{Cu}} = 25\ \mathrm{nm}^{-1}$,[36] we obtain lifetimes of the same order of magnitude as the experiment, that increase towards the band bottom. This can be understood by a simple phase-space argument. When approaching the band minimum, the number of final states for intraband scattering processes decreases, so that an electron at the band bottom can only relax its energy by an interband scattering process. Consequently, the states at the band bottom have the longest lifetimes. The monotonically increasing behavior of the calculated result around the intersection point is due to a special property of the Rashba model: the spin mixing is independent of the magnitude of k and the spin expectation values are always in-plane. Taken together, this implies that there is no pronounced momentum dependence of the spin-flip scattering around the band intersection point. This is in good agreement with the findings of Nechaev *et al.*, who investigated the inelastic hole lifetimes in the Rashba spin-orbit split surface state of Au(111) and also found that the lifetime behavior in both branches does not deviate much from the behavior that is expected in simple parabolic electronic bands.[37] Hence, the calculated lifetimes for a pure Rashba system deviate from experiment around the intersection point.

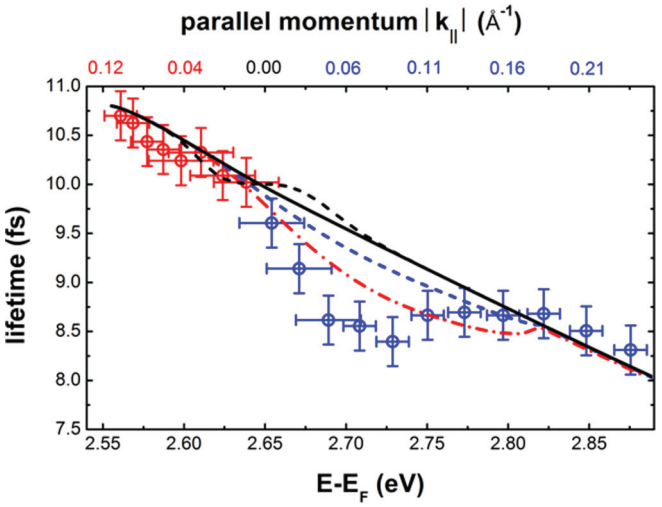

FIG. 3. (Color online) Calculated (lines) and measured lifetimes (red circles and blue circles for below and above the intersection point located at about $E - E_F = 2.65$ eV, respectively). The increased error bars around the intersection point account for the uncertainty due to limited experimental energy resolution. Note, however, that all extracted data points are well separated in $k_\parallel$ space [c.f. Fig. 1(b)]. The black line corresponds to a pure Rashba model with experimental parameters. The black dashed line illustrates the maximum deviation that might be introduced by the limited experimental energy resolution. In the results represented by the red (dash-dotted) and blue (dotted) lines, an additional spin-mixing is included (see text).

First, we want to investigate if the limited energy resolution in our time-resolved 2PPE experiment ($\Delta E = 100$ meV) might artificially induce the peculiar lifetime behavior seen in the experimental data. If the energy resolution is not sufficient to separately resolve the two spin-split bands towards the intersection point, the extracted electron lifetimes in the upper and lower branch constitute a convolution of lifetimes within the given energy resolution. We therefore have included the limited energy resolution in our theoretical model, and the black dashed line in Fig. 3 displays the maximum effect of the limited energy resolution on the extracted electron lifetimes. Clearly, these deviations are minor in comparison to the experimentally observed behavior.

As discussed above, we have seen that the band-structure-dependent intraband-scattering rate dominates the observed dynamics in this electronic system, which is expected, and also in agreement with previous studies.[14,20–22] Following this line of reasoning, we conclude that the decrease of lifetimes around the intersection point of the Rashba bands is also most likely determined by a variation in the intraband-scattering rate. Additionally, we recognize that a less exact Rashba-type spin texture would directly induce such a behavior, since most intraband scattering processes would not need to involve spin flips anymore. We therefore suggest here that the spin texture of the Bi/Cu(111) system may be not purely Rashba-like, i.e., spin-orbit coupling effects beyond those described in a pure Rashba model must play a role to induce the experimentally observed decrease in electron lifetimes around the intersection point. Note that deviations from a pure Rashba-type spin texture, and in particular out-of-plane components, have been observed in various other material systems before.[38–41]

E. Implication of spin-mixing

We now want to focus on our theoretical model and its relation to the experimentally observed decreased lifetimes in the vicinity of the Rashba intersection point. It seems very likely that an increased probability of intraband-scattering processes between the spin-split bands would directly lead to a behavior of the calculated lifetimes closer to the one experimentally observed. As mentioned above, the k independence of the Rashba spin mixing is the reason for the monotonic increase of lifetimes towards the band bottom. We therefore test now how deviations from a pure Rashba system would influence the electron lifetimes. In theory, this is most easily achieved by the introduction of an additional spin-mixing that leads to an out-of-plane spin component. Note that the spin-mixing is introduced here in an *ad-hoc* fashion to mimic a nontrivial spin structure at the intersection point, while the dispersion of the bands is left unchanged; in particular, no band gap is included. We consider states of the form

$$\widetilde{|\mathbf{k},\sigma\rangle} = \frac{\beta(k)}{\sqrt{2}}\begin{pmatrix}\sigma i e^{-i\varphi_{\mathbf{k}}}\\ 1\end{pmatrix} + \frac{\sqrt{1-\beta^2(k)}}{\sqrt{2}}\begin{pmatrix}-\sigma i e^{-i\varphi_{\mathbf{k}}}\\ 1\end{pmatrix}. \quad (19)$$

Here, we have introduced a mixing parameter $\beta(k) \in [\frac{1}{\sqrt{2}},1]$. For $\beta(k) = \frac{1}{\sqrt{2}}$, the spin mixing is maximal and the expectation value of spin in the xy plane is zero. A direct consequence of the k-dependent spin mixing is that the overlaps between these states are different from those in the pure Rashba model. With the definitions $\beta(k) = \beta_1$ and $\beta(|\mathbf{k}+\mathbf{q}|) = \beta_2$, one obtains

$$\begin{aligned}\tilde{M}^{\sigma,\mu}_{\mathbf{k},\mathbf{q}} &= \beta_1^2\beta_2^2 M^{\sigma,\mu}_{\mathbf{k},\mathbf{q}} + \beta_1^2(1-\beta_2^2)M^{\sigma,-\mu}_{\mathbf{k},\mathbf{q}}\\ &\quad + (1-\beta_1^2)\beta_2^2 M^{-\sigma,\mu}_{\mathbf{k},\mathbf{q}} + (1-\beta_1^2)(1-\beta_2^2)M^{-\sigma,-\mu}_{\mathbf{k},\mathbf{q}}\\ &\quad + 2\beta_1\beta_2\sqrt{1-\beta_1^2}\sqrt{1-\beta_2^2}. \end{aligned} \quad (20)$$

The simplest assumption for the mixing parameter is a linear k dependence away from the crossing point,

$$\beta(k) = \begin{cases}\frac{1}{\sqrt{2}} + \frac{1}{k_c}\left(1-\frac{1}{\sqrt{2}}\right)k, & k < k_c,\\ 1, & k > k_c,\end{cases} \quad (21)$$

in a limited range of $\mathbf{k}$ vectors around the crossing point $\mathbf{k} = 0$. Note that this yields a maximal spin mixing at the intersection point, which means that the spin points out of the xy plane. The mixing decreases with increasing k and for $k > k_c$, we have a Rashba splitting without additional mixing. If we replace $\frac{1}{\sqrt{2}}$ by a larger numerical value in Eq. (21), we do not get total spin mixing at the crossing point. For instance, $\beta(0) = 0.91$ leads to an out-of-plane spin component of $0.75\frac{\hbar}{2}$. This spin-mixing model makes the vicinity of the crossing point into a spin hot spot, where strong spin mixing at specific points in the electronic band structure is assumed to enable efficient spin-flip scattering processes.[11,12]

Figure 3 shows results calculated with spin mixing as in Eq. (21) with $k_c = 0.7\ \mathrm{nm}^{-1}$. The blue (dashed) curve corresponds to a maximum out-of-plane spin component of $0.75\frac{\hbar}{2}$ and the red (dash-dotted) curve to a maximum out-of-plane spin of $\frac{\hbar}{2}$. These calculated results resemble the increased decay rate around the intersection as observed in experiment. Clearly, with increasing mixing parameter, the process of intraband scattering in the vicinity of the intersection point becomes more efficient and the measured lifetimes consequently decrease. Although these results do point in the same direction as the experimental results, our finding is no rigorous proof of such a spin hot spot scenario. However, we do not see any other decay channel that could be responsible for such strong variations in the electron lifetimes in this system. Finally, we want to add that the strength of the spin mixing necessary to resemble the experimental data is quite large, which leads to a pronounced deviation from a pure Rashba-like spin structure. Such a deviation should be observable and seems to be in agreement with recent experimental and theoretical results on the "orbital Rashba splitting".[42,43]

IV. CONCLUSION

In summary, we presented a detailed experimental and theoretical investigation of the influence of spin-orbit coupling on the electronic lifetimes. The experimental data and the calculated lifetimes for a pure Rashba model showed the expected Fermi-liquid behavior with an increase of the electron lifetimes towards the band bottom of the spin-split bands. The experimental results, however, additionally showed a pronounced decrease in the lifetimes just above the intersection of the split bands, which is not compatible with a pure Rashba model calculation. We suggested that spin-orbit coupling effects beyond those described in a pure Rashba model might play a role in the Bi/Cu(111) system. Consequently, we considered a deviation from a perfect Rashba spin mixing in our theoretical model that leads to out-of-plane spin components and makes the band crossing into a spin hot spot. Constructing such a spin texture with out-of-plane components from the Rashba bands resembles the characteristic features of the experiment better, which is an indication that spin mixing indeed might induce the decreased lifetimes at the intersection point.

ACKNOWLEDGMENTS

We thank T. Stroucken (Marburg) for helpful discussion regarding the treatment of the screened potential. We are grateful to the Jülich Supercomputer Centre (JSC) for a CPU-time grant. This work was supported by the Excellence Initiative DFG/GSC 266 (S.J.).

*smathias@physik.uni-kl.de

[1] Y. Bychkov and E. Rashba, JETP Lett. **39**, 78 (1984).
[2] J. Stajic, Science **333**, 1680 (2011).
[3] C. R. Ast, J. Henk, A. Ernst, L. Moreschini, M. C. Falub, D. Pacilé, P. Bruno, K. Kern, and M. Grioni, Phys. Rev. Lett. **98**, 186807 (2007).

[4]S. Mathias, A. Ruffing, F. Deicke, M. Wiesenmayer, I. Sakar, G. Bihlmayer, E. V. Chulkov, Y. M. Koroteev, P. M. Echenique, M. Bauer, and M. Aeschlimann, Phys. Rev. Lett. **104**, 066802 (2010).
[5]S. Jakobs, A. Ruffing, M. Cinchetti, S. Mathias, and M. Aeschlimann, Phys. Rev. B **87**, 235438 (2013).
[6]J. H. Dil, F. Meier, J. Lobo-Checa, L. Patthey, G. Bihlmayer, and J. Osterwalder, Phys. Rev. Lett. **101**, 266802 (2008).
[7]P. D. C. King, R. C. Hatch, M. Bianchi, R. Ovsyannikov, C. Lupulescu, G. Landolt, B. Slomski, J. H. Dil, D. Guan, J. L. Mi, E. D. L. Rienks, J. Fink, A. Lindblad, S. Svensson, S. Bao, G. Balakrishnan, B. B. Iversen, J. Osterwalder, W. Eberhardt, F. Baumberger, and Ph. Hofmann, Phys. Rev. Lett. **107**, 096802 (2011).
[8]A. Crepaldi, L. Moreschini, G. Autès, C. Tournier-Colletta, S. Moser, N. Virk, H. Berger, Ph. Bugnon, Y. J. Chang, K. Kern, A. Bostwick, E. Rotenberg, O. V. Yazyev, and M. Grioni, Phys. Rev. Lett. **109**, 096803 (2012).
[9]G. Landolt, S. V. Eremeev, Y. M. Koroteev, B. Slomski, S. Muff, T. Neupert, M. Kobayashi, V. N. Strocov, T. Schmitt, Z. S. Aliev, M. B. Babanly, I. R. Amiraslanov, E. V. Chulkov, J. Osterwalder, and J. H. Dil, Phys. Rev. Lett. **109**, 116403 (2012).
[10]S. V. Eremeev, I. A. Nechaev, Y. M. Koroteev, P. M. Echenique, and E. V. Chulkov, Phys. Rev. Lett. **108**, 246802 (2012).
[11]J. Fabian and S. Das Sarma, Phys. Rev. Lett. **81**, 5624 (1998).
[12]M. Pickel, A. B. Schmidt, F. Giesen, J. Braun, J. Minár, H. Ebert, M. Donath, and M. Weinelt, Phys. Rev. Lett. **101**, 066402 (2008).
[13]M. Hengsberger, F. Baumberger, H. J. Neff, T. Greber, and J. Osterwalder, Phys. Rev. B **77**, 085425 (2008).
[14]S. Mathias, A. Ruffing, F. Deicke, M. Wiesenmayer, M. Aeschlimann, and M. Bauer, Phys. Rev. B **81**, 155429 (2010).
[15]We use standard picture panorama software to merge the full-angle distribution photoemission maps from several individual measurements. In the process of merging, the data are slightly corrected for lens distortions and intensity deviations. Therefore all physical quantities shown in our paper are extracted from the original data sets.
[16]H. Petek and S. Ogawa, Prog. Surf. Sci. **56**, 239 (1997).
[17]J. P. Gauyacq and A. K. Kazansky, Phys. Rev. B **72**, 045418 (2005).
[18]F. Steeb, S. Mathias, A. Fischer, M. Wiesenmayer, M. Aeschlimann, and M. Bauer, New J. Phys. **11**, 013016 (2009).
[19]P. S. Kirchmann, L. Rettig, X. Zubizarreta, V. M. Silkin, E. V. Chulkov, and U. Bovensiepen, Nat. Phys. **6**, 782 (2010).
[20]W. Berthold, U. Hofer, P. Feulner, E. V. Chulkov, V. M. Silkin, and P. M. Echenique, Phys. Rev. Lett. **88**, 056805 (2002).
[21]M. Rohleder, K. Duncker, W. Berthold, J. Güdde, and U. Höfer, New J. Phys. **7**, 103 (2005).
[22]K. Schubert, A. Damm, S. V. Eremeev, M. Marks, M. Shibuta, W. Berthold, J. Güdde, A. G. Borisov, S. S. Tsirkin, E. V. Chulkov, and U. Höfer, Phys. Rev. B **85**, 205431 (2012).
[23]M. Bauer, S. Pawlik, and M. Aeschlimann, Phys. Rev. B **60**, 5016 (1999).
[24]H. Ueba and B. Gumhalter, Prog. Surf. Sci. **82**, 193 (2007).
[25]A. Zugarramurdi, N. Zabala, V. M. Silkin, A. G. Borisov, and E. V. Chulkov, Phys. Rev. B **80**, 115425 (2009).
[26]M. Wiesenmayer, M. Bauer, S. Mathias, M. Wessendorf, E. V. Chulkov, V. M. Silkin, A. G. Borisov, J. P. Gauyacq, P. M. Echenique, and M. Aeschlimann, Phys. Rev. B **78**, 245410 (2008).
[27]T. Fauster, *Dynamics at Solid State Surfaces and Interfaces* (Wiley, New York, 2010), pp. 53–73.
[28]S. Mathias, S. V. Eremeev, E. V. Chulkov, M. Aeschlimann, and M. Bauer, Phys. Rev. Lett. **103**, 026802 (2009).
[29]S. Mathias, M. Wiesenmayer, M. Aeschlimann, and M. Bauer, Phys. Rev. Lett. **97**, 236809 (2006).
[30]L. Zheng and S. Das Sarma, Phys. Rev. B **53**, 9964 (1996).
[31]G. F. Giuliani and J. J. Quinn, Phys. Rev. B **26**, 4421 (1982).
[32]V. S. Edel'man, Phys. Usp. **48**, 1057 (2005).
[33]I. A. Nechaev, V. M. Silkin, and E. V. Chulkov, J. Exp. Theor. Phys. **112**, 134 (2011).
[34]G. Giuliani and G. Vignale, *Quantum Theory of the Electron Liquid* (Cambridge University Press, Cambridge 2005).
[35]G. D. Mahan, *Many-Particle Physics* (Springer, Berlin, 2000).
[36]S. Ogawa, H. Nagano, and H. Petek, Phys. Rev. B **55**, 10869 (1997).
[37]I. A. Nechaev, M. F. Jensen, E. D. L. Rienks, V. M. Silkin, P. M. Echenique, E. V. Chulkov, and P. Hofmann, Phys. Rev. B **80**, 113402 (2009).
[38]T. Okuda, K. Miyamaoto, Y. Takeichi, H. Miyahara, M. Ogawa, A. Harasawa, A. Kimura, I. Matsuda, A. Kakizaki, T. Shishidou, and T. Oguchi, Phys. Rev. B **82**, 161410 (2010).
[39]A. Takayama, T. Sato, S. Souma, and T. Takahashi, J. Vac. Sci. Technol. B **30**, 04E107 (2012).
[40]K. Ishizaka, M. S. Bahramy, H. Murakawa, M. Sakano, T. Shimojima, T. Sonobe, K. Koizumi, S. Shin, H. Miyahara, A. Kimura, K. Miyamoto, T. Okuda, H. Namatame, M. Taniguchi, R. Arita, N. Nagaosa, K. Kobayashi, Y. Murakami, R. Kumai, Y. Kaneko, Y. Onose, and Y. Tokura, Nat. Mater. **10**, 521 (2011).
[41]P. Höpfner, J. Schäfer, A. Fleszar, J. H. Dil, B. Slomski, F. Meier, C. Loho, C. Blumenstein, L. Patthey, W. Hanke, and R. Claessen, Phys. Rev. Lett. **108**, 186801 (2012).
[42]S. R. Park, C. H. Kim, J. Yu, J. H. Han, and C. Kim, Phys. Rev. Lett. **107**, 156803 (2011).
[43]J.-H. Park, C. H. Kim, J.-W. Rhim, and J. H. Han, Phys. Rev. B **85**, 195401 (2012).